QCD critical point and complex chemical potential singularities

M. A. Stephanov

Department of Physics, University of Illinois, Chicago, Illinois 60607-7059, USA

(Received 3 April 2006; published 22 May 2006)

The thermodynamic singularities of QCD in the plane of *complex* baryo-chemical potential μ are studied. Predictions are made using scaling and universality arguments in the vicinity of the massless quark limit. The results are illustrated by a calculation of complex μ singularities in a random matrix model at finite temperature. Implications for lattice QCD simulations aimed at locating the QCD critical point are discussed.

DOI: 10.1103/PhysRevD.73.094508 PACS numbers: 12.38.Gc, 12.38.Mh, 64.60.Fr

I. INTRODUCTION

The search for the QCD critical point has attracted considerable theoretical and experimental attention recently. The existence of such a point—an ending point of the first order chiral transition in QCD—was suggested a long time ago [1,2], and the properties were studied using universality arguments and model calculations more recently [3,4] (see Ref. [5] for review). The experimental search for the critical point using heavy ion collisions has been proposed in [6]. It is apparent that theoretical knowledge of the location of the critical point on the phase diagram is important for the success of the experimental search.

First principle lattice QCD calculations aimed at determining the location of the critical point on the T, μ (temperature, baryon-chemical potential) diagram have been attempted recently using several different techniques [7–10] (see Ref. [11] for review). The major obstacle for direct Monte Carlo simulation is the well-known lack of positivity of the measure of the path integral defining QCD partition function at nonzero baryo-chemical potential μ—the sign problem. One of the methods to deal with this problem is to Taylor expand the QCD pressure in powers of μ around $\mu = 0$, i.e., around the point at which direct Monte Carlo simulations are not hindered by the sign problem [8,10].

The success of such an approach in determining the location (T_E, μ_E) of the critical ending point crucially depends on the convergence radius of the Taylor expansion around $\mu = 0$ [8,10,12]. The convergence radius, in turn, is a function of the position of the singularities in the complex μ plane. Little is known about the location of these singularities to date. The purpose of this paper is to expand our knowledge of the location of these complex plane singularities.

We shall be able to determine the position of the singularities in the regime where the quark masses m are sufficiently small. To summarize, the strongest rigorous consequence of our analysis is that the convergence radius, μ_R, achieves its minimum value at a temperature slightly above T_c (by $\mathcal{O}(m^{1/(\beta\delta)})$). This value scales as

$$\min_T \mu_R(T) \sim m^{1/(2\beta\delta)}, \tag{1}$$

and vanishes in the chiral limit ($m \to 0$). The value $1/(\beta\delta) \approx 0.54$ is determined by the critical exponents of the O(4) universality class in 3 dimensions. The singularity which determines the radius in (1) lies in the complex plane and pinches the real axis (together with its conjugate) at the critical point. The convergence radius $\mu_R(T)$ has a certain nonanalyticity at $T = T_E$, which we shall describe.

The study of thermodynamic singularities, or partition function zeros, in the complex plane was pioneered by Yang and Lee [13]. Their analysis was extended by Fisher from the complex magnetic field singularities to complex temperature singularities [14]. The properties of these singularities following from scaling and universality have been further studied by Fisher [15], Itzykson, Pearson and Zuber [16] and others.

From the point of view of the lattice studies of the QCD phase diagram, we would like to distinguish two separate issues. One is the convergence of the series as the truncation order is increased. This is the issue which this study will impact. The other is the convergence of each term in the series to its thermodynamic limit as the volume and/or the number of Monte Carlo configurations are increased. The sign-problem is affecting this latter convergence and will not be addressed here (see, e.g., [17–19]).

II. UNIVERSAL PROPERTIES OF THE COMPLEX SINGULARITIES

Here we describe generic universal properties of the complex thermodynamic singularities. The basic results following from scaling and universality are not new, and can be found in [16]. For clarity and completeness, we rederive the needed facts here using slightly different approach. Our purpose is to apply these results to QCD at finite temperature and density.

A. Complex μ singularities as Fisher zeros

We shall first consider QCD in the chiral limit—the limit of two lightest quark masses taken to zero. The phase diagram in the (T, μ) plane is sketched in Fig. 1. The low-

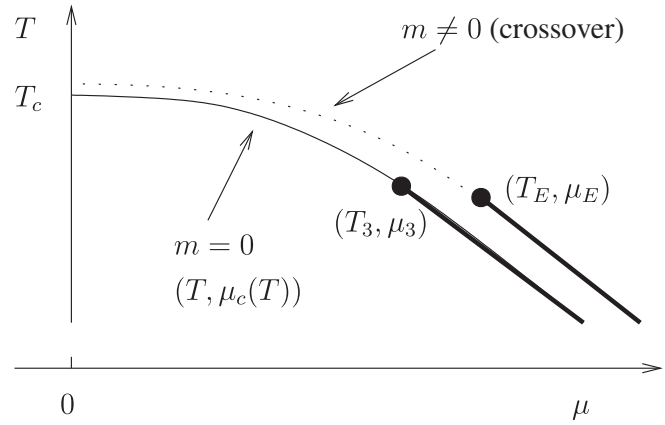

FIG. 1. A sketch of the QCD phase diagram in the vicinity of the critical line $\mu_c(T)$ for zero and nonzero quark mass.

temperature phase is separated from the high-temperature phase by a phase transition. This is unavoidable, because the symmetry of the ground state must change from $SU(2)_V \times U(1)_B$ to the full symmetry of the action $SU(2)_V \times SU(2)_A \times U(1)_B$ as the temperature is raised [20]. This transition is of second order for $\mu < \mu_3$, and of first order for $\mu > \mu_3$.

Let us now fix T at a value in the interval (T_3, T_c) and study the behavior of singularities in the complex μ plane. On the real axis, as μ increases from zero, the transition occurs at a value which we denote as $\mu_c(T)$ (see Fig. 1). Therefore, at a fixed temperature, the change of the chemical potential $\mu - \mu_c(T)$ is a relevant perturbation. In the universality class of the $O(3) \to O(4)$ transitions, to which QCD chiral restoration transition belongs [21], there is only one relevant variable—the thermal variable t (we are discussing the symmetry limit—the magnetic field variable h is absent). Therefore, we are led to consider the universal behavior of the singularities in the complex *temperature* plane, which correspond to Fisher zeros. The scaling parameter t is to linear order

$$t \sim \mu^2 - \mu_c{}^2(T). \tag{2}$$

We use μ^2 instead of μ to ensure that at $\mu = 0$ the thermal variable is proportional to $T - T_c$.

B. Partition function zeros and electrostatic analogy

As first exposed by Lee and Yang [13], the thermodynamic singularities in the complex plane are related to the zeros of the partition function. For a finite system the partition function Z, by definition, is strictly positive for *real* values of the parameters. However, Z has zeros in the complex plane, whose number grows linearly with the size of the system. In the thermodynamic limit the zeros typically coalesce into cuts. A phase transition occurs where such a cut pinches (second order) or crosses (first order) the real axis.

The considerations of Lee and Yang apply to the variable $\lambda \equiv \exp(\mu/T)$ since the partition function of QCD is a polynomial (times an integer power) in λ due to quantization of the baryon charge. It is convenient to use the electrostatic analogy. The partition function—a polynomial, can be written in terms of its roots

$$Z(\lambda) = \prod_k (\lambda - \lambda_k). \tag{3}$$

Therefore the free energy (or grand potential, if we are dealing with grand canonical ensemble, as in QCD) is

$$\Omega(\lambda) = -T \log Z = -T \sum_k \log(\lambda - \lambda_k). \tag{4}$$

For complex λ, the real part $\mathrm{Re}\Omega$ can be interpreted as an electrostatic potential created by charges located on the plane $(\mathrm{Re}\lambda, \mathrm{Im}\lambda)$:

$$\mathrm{Re}\,\Omega(\lambda) = -T \sum_i \log|\lambda - \lambda_k|. \tag{5}$$

All charges have the same magnitude and sign (degenerate roots can be treated as coincident charges). Now let us assume, as is known to be true in most cases, and in the universality region of interest, in particular, that the zeros coalesce into 1-dimensional curves in the thermodynamic limit. Then, the electrostatic potential $\mathrm{Re}\Omega$ is continuous across such a curve, while the analog of the electric field

$$\boldsymbol{E} = -\boldsymbol{\nabla}(\mathrm{Re}\Omega) = -\left(\frac{\partial\,\mathrm{Re}\Omega}{\partial\,\mathrm{Re}\lambda}, \frac{\partial\,\mathrm{Re}\Omega}{\partial\,\mathrm{Im}\lambda}\right) = (-\mathrm{Re}, \mathrm{Im})\frac{d\Omega}{d\lambda} \tag{6}$$

is discontinuous—the normal component jumps by an amount proportional to the linear charge density ρ on the curve. This curve can be viewed as the location of a cut on a Riemann sheet of the analytic function $\Omega(\lambda)$.

C. Stokes boundaries in the scaling region at $h = 0$

Consider now the critical region in the vicinity of a critical point λ_c. In the scaling regime the singular (i.e., nonanalytic) part of the potential $\Omega(t)$ is proportional to a power of t:

$$\Omega_{\mathrm{sing}}(t) = \begin{cases} A_+ t^{2-\alpha}, & t > 0; \\ A_-(-t)^{2-\alpha}, & t < 0; \end{cases} \qquad t \equiv \frac{\lambda - \lambda_c}{\lambda_c} \tag{7}$$

which defines the universal specific heat exponent α and the amplitudes $A_\pm$, whose ratio is also universal. Off the real axis $\Omega(t)$ must be an analytic function everywhere except for discontinuities across the cuts. Such cuts (at least two, by symmetry $\Omega(t^*) = \Omega(t)$) must be present, because the function (7) taken at $t > 0$ does not match its analytic continuation from the $t < 0$ axis along a path around $t = 0$. The location of the cuts can be determined using electrostatic analogy, which requires $\mathrm{Re}\Omega$ to be continuous across the cut. Parameterizing $t = -se^{i\varphi}$ using real parameter $s > 0$ we find:

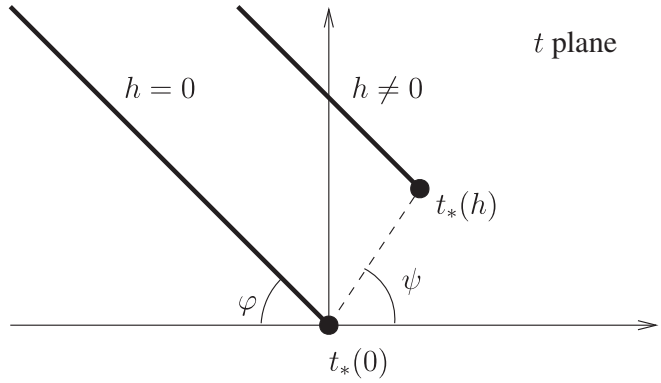

FIG. 2. Universal behavior of Stokes boundaries in the scaling region for zero and nonzero symmetry breaking parameter h. Only upper complex half-plane is shown. The trajectory of the branching point $t_*(h)$ is indicated by a dashed line.

$$A_+ \cos[(2-\alpha)(\varphi-\pi)] = A_- \cos[(2-\alpha)\varphi]. \tag{8}$$

Therefore, the cuts are straight lines at an angle with respect to the negative t axis given by (cf. [16])

$$\tan[(2-\alpha)\varphi] = \frac{\cos(\pi\alpha) - A_-/A_+}{\sin(\pi\alpha)}, \tag{9}$$

as shown in Fig. 2. All quantities entering this formula are universal.

The cuts are termed Stokes boundaries in [16]—they carry conceptual resemblance to the anti-Stokes lines in the WKB theory. Across these lines, the function Ω switches from one of its Riemann sheets to another. The density of the "charges" on the cut is proportional to the discontinuity of the normal component of $\boldsymbol{E}$, and thus to $\mathrm{Im}(e^{i\varphi} d\Omega/dt)$, which vanishes at the branching point as

$$\rho \sim |t|^{1-\alpha}. \tag{10}$$

D. Stokes boundaries at $h \neq 0$

The magnetic field h is another relevant variable near the O(4) critical point. The magnetic field breaks the O(4) down to O(3), and in QCD this role is played by the quark mass m (more precisely, the average of the u and d masses). At $h \neq 0$ the free energy is analytic function of t at $t = 0$. In the scaling region the singular part of the free energy scales as a power of h if t is also changed to keep the scaling variable $x \equiv th^{-1/(\beta\delta)}$ fixed. Therefore the (two) branching points must be located at a point away from the origin given by

$$t_* = x_* h^{1/(\beta\delta)} \tag{11}$$

and at $(t_*)^*$, where x_* is a complex constant. The phase of t_* (the polar angle coordinate of the branching point) is determined by the following argument. By scaling postulate, the singular contribution to the free energy must be given by

$$\Omega_{\mathrm{sing}} = h^{1+1/\delta} A(th^{-1/(\beta\delta)}) \tag{12}$$

where the function $A(x)$ is analytic at $x = 0$. $A(x)$ has two cuts which originate at points x_* and $(x_*)^*$ and go off to infinity. Consider Ω_{sing} as a function of *complex* h at fixed real t. By symmetry ($h \leftrightarrow -h$, $h \leftrightarrow h^*$), the Stokes boundaries of this function lie on the imaginary axis (more rigorously, this follows from the Lee-Yang theorem and universality). Thus the branching point, for $t > 0$, at $h_* = (t/x_*)^{\beta\delta}$, is purely imaginary, and therefore $\beta\delta \arg x_* = \pi/2$. Thus,

$$t_* = |x_*| e^{i\psi} h^{1/(\beta\delta)}, \qquad \psi = \frac{\pi}{2\beta\delta}. \tag{13}$$

To summarize, at $h = 0$, the complex singularities in the scaling region of the thermal parameter t form cuts (Stokes boundaries) which go along the rays at angle φ with the negative real axis given by (9). With increasing symmetry breaking parameter h the branching point shifts away from $t = 0$ by an amount proportional to $h^{1/(\beta\delta)}$ along the direction at the angle ψ to the positive t axis given by (13). This is illustrated in Fig. 2.

III. SINGULARITIES OF QCD IN THE COMPLEX μ PLANE

A. Chiral limit: $m = 0$

Let us begin with the chiral limit $m = 0$. Consider the interval of $T \in (T_3, T_c)$. In this interval increasing μ leads to the second order transition at $\mu = \mu_c(T)$. As discussed in the previous section in the vicinity of the transition we must identify t with $\mu^2 - \mu_c{}^2(T)$ (up to an irrelevant constant factor)—Eq. (2). Thus, at a given temperature T, near $\mu_c(T)$ the location of the singularities in the complex μ plane is determined by the universal arguments of the previous section. Conformal transformation $\mu \to \mu^2$ does not affect the angles ϕ and ψ away from $\mu = 0$.

In particular, at $m = 0$, the (two) cuts should originate at the branching point located at $\mu_c(T)$ on the real axis, and follow the rays at angle φ given by (9) with respect to the negative real axis as shown in Fig. 3 (left).

Taking the values $\alpha \approx -0.25$ [22] and $A_+/A_- \approx 1.6$ [23] we estimate the value of the angle as $\varphi \approx 77°$. At the tricritical point $\alpha = 1/2$ and $A_+/A_- = 0$ and thus $\varphi = 60°$.

B. Small quark mass: $m \neq 0$

At finite quark mass m the second order line $\mu = \mu_c(T)$ is replaced by an analytic crossover for all temperatures $T > T_E$. The critical ending point of the first order transition is located at a temperature we denote T_E. For $T < T_E$ the transition is of the first order.

At fixed $T > T_3$, and small mass m, in the vicinity of the crossover point the singularities are described by the uni-

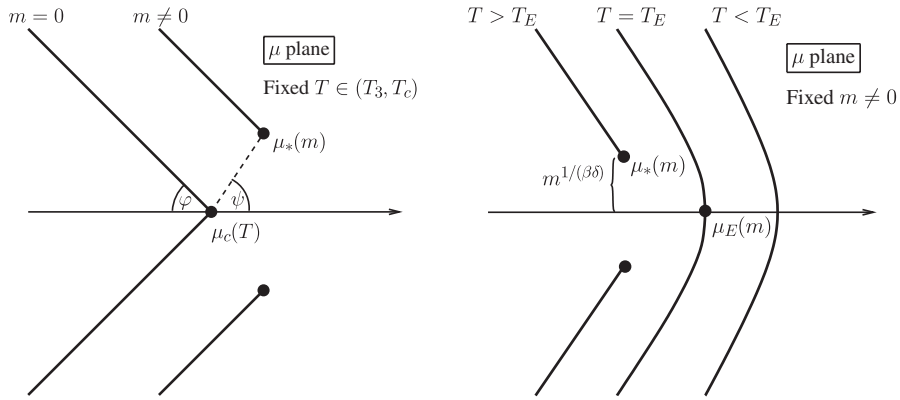

FIG. 3. Stokes boundaries in QCD at fixed T and two different values of m (left) and at fixed small m and three different values of T (right) as dictated by universality.

versal arguments with

$$h \sim m. \tag{14}$$

For the purpose of the discussion we can define the crossover point as the value of the real part of the branching point: $\mu_{\text{crossover}} \equiv \text{Re}(\mu_*(m))$. The branching point, $\mu_*(m)$ or the nearest singularity to the real axis, is shifted by the amount proportional to $m^{1/(\beta\delta)}$, which is $m^{0.54}$, using the O(4) critical exponents [22], in the direction along the ray at angle (13) $\psi = \pi/(2\beta\delta) \approx 48°$ towards the positive real axis as shown in Fig. 3 (left).

When T is decreased towards T_E this branching point $\mu_*(m)$ (and its conjugate) approach the real axis and pinch it when $T = T_E$. At this temperature, the cuts originate from the branching point on the real axis μ_E (see Fig. 3 (right)). The point (T_E, μ_E) is the QCD critical ending point. This ordinary critical point is in the universality class of the Ising model [3,4]. The initial direction of the cuts near this point is perpendicular to the real axis, i.e., $\varphi = 90°$. This follows from the fact that the perturbation $\mu - \mu_E$ is magnetic-field-like,

$$h \sim \mu - \mu_E, \tag{15}$$

and from the fact that singularities in the h plane lie on the imaginary axis.

The reason that $\mu - \mu_E$ is not t-like, but h-like, is the following. In the vicinity of the critical point, since the O(4) is explicitly broken, the perturbation $\mu - \mu_E$ affects both the thermal variable t as well as magnetic-field-like variable h to linear order. Since $\beta\delta > 1$, the scaling variable $x = th^{-1/(\beta\delta)}$ is small, which means the perturbation $\mu - \mu_E$ takes the system into the region where the variable h dominates the scaling.[1]

[1]An equivalent way of saying this is by comparing the scaling dimensions of the variables coupled to thermal and magnetic relevant operators: $y_t = 1/\nu$ and $y_h = \beta\delta/\nu$. Since both operators couple linearly to the variable $\mu - \mu_E$, and $y_h > y_t$, the magnetic field operator dominates the response to $\mu - \mu_E$ perturbation near the critical point. In contrast, at $m = 0$, the coupling to magnetic operator is forbidden by symmetry.

IV. RANDOM MATRIX MODEL

In this section we illustrate the universal properties discussed above by determining the complex plane singularities of a random matrix model of the QCD partition function at finite T and μ which was introduced in Ref. [4] and applied to the study of the QCD phase diagram and the (tri)critical point. At $\mu = 0$ this model is equivalent to the finite-T model of Ref. [24] and at $T = 0$—to the finite-μ model of Ref. [25]. The parameters T, μ and m used in this section are dimensionless, and correspond to measuring T in units of $T_c = 160$ MeV, μ in units of 2.27 GeV, and m in units of 100 MeV. For more details, see Ref. [4].

The model can be solved in the thermodynamic limit, which corresponds to the infinite size of the random matrix, $N \to \infty$, by using the replica trick. This gives, for real μ, T and m,

$$\log Z_{\text{RM}} = -\min_{\phi} \Omega(\phi) \tag{16}$$

where

$$\Omega(\phi) = \phi^2 - \tfrac{1}{2}\ln\{[(\phi + m)^2 - (\mu + iT)^2] \cdot [(\phi + m)^2 - (\mu - iT)^2]\}. \tag{17}$$

Analytically continuing into the complex μ-plane, one finds the branching points of the partition function by solving a system of two algebraic equations

$$\frac{d\Omega}{d\phi} = 0; \qquad \frac{d^2\Omega}{(d\phi)^2} = 0 \qquad \text{(branching points)} \tag{18}$$

for two unknowns: ϕ and μ. The second equation states that two of the solutions determined by the first equation are coalescing into one at this value of μ. The Stokes boundaries can be determined by solving the condition $\text{Re}\Omega(\phi_1) = \text{Re}\Omega(\phi_2)$ where ϕ_1 and ϕ_2 are the two solutions of the first equation in (18) which coalesce at the

branching point:

$$\frac{d\Omega}{d\phi}\bigg|_{\phi=\phi_1,\phi_2} = 0; \qquad \mathrm{Re}\Omega(\phi_1) = \mathrm{Re}\Omega(\phi_2). \tag{19}$$

(Stokes boundaries).

At *finite* N the partition function can be written explicitly as a polynomial (apart from an irrelevant constant factor)

$$Z_{\mathrm{RM}}^{(N)} = \sum_{k_1,k_2=0}^{N/2} \binom{N}{k_1}\binom{N}{k_2}(N-k_1-k_2)!\,{}_1F_1(k_1+k_2 - N; 1; -m^2N)[-(\mu+iT)^2N]^{k_1}[-(\mu-iT)^2N]^{k_2}, \tag{20}$$

using the procedure similar to [26], where ${}_1F_1(a;b;c)$ is the Kummer confluent hypergeometric function (in (20) it is a polynomial in m^2). The zeros are found numerically for $N = 120$ and plotted in Fig. 4 together with the Stokes boundaries given by (19).

Near the point $T = T_c$, $\mu = 0$, the thermal scaling variable t is proportional to $(T - T_c) + C\mu^2$, where C is the constant giving the slope the second order transition curve (see Eq. (2)). Therefore it is convenient to plot the zeros in the complex μ^2 plane.

Only the vicinity of the origin $\mu^2 = 0$ is shown in Fig. 4. The universal properties described in the previous section are manifest. It is clear from the form of the solution (16) that the critical exponents near the second order line have their mean field values, and correspondingly, the angles are $\varphi = 45°$ and $\psi = 60°$. At the tricritical point, the exponents are given by their mean field values also in QCD (albeit with logarithmic corrections): $\varphi = 60°$, $\psi = 72°$. One can also see that the density of the zeros decreases near the branching point, as dictated by (10).

V. CONVERGENCE RADIUS

Relevant for the search of the QCD critical point is the question of the convergence radius $\mu_R^2(T)$ of the Taylor expansion around $\mu = 0$ of the QCD thermodynamic potential as a function of T. For sufficiently small quark masses, and sufficiently near T_c, the position of the nearest singularity, limiting this radius, is determined by the universal arguments given above. For illustration, this radius in the random matrix model is plotted on Fig. 5.

All generic and universal features are manifest in Fig. 5. As T decreases, and the branching point singularity slides along the dashed line on Fig. 4 from left to right, the radius μ_R contracts, and then, below the crossover temperature, begins to expand again. From the universality arguments of Sec. III (see Fig. 3 (right)) we conclude that near the chiral ($m \to 0$) limit the minimum value of the radius scales with m as

$$\min_T \mu_R^2(T) \sim m^{1/(\beta\delta)} \sim m^{0.54}, \tag{21}$$

and is achieved at a temperature T which scales as $T - T_c \sim m^{1/(\beta\delta)} \sim m^{0.54}$.

Further away from the minimum, at the critical point, $T = T_E$, the singularity and its conjugate pinch the real axis. At this point one observes a nonanalyticity in $\mu_R^2(T)$: a contribution of order $(T_E - T)^{\beta\delta}$ turns on below $T = T_E$. This is due to the kink in the dashed line on Fig. 4 at T_E. In QCD $\beta\delta \approx 1.56$, given by the exponents of the 3d Ising model, while in the random matrix model $\beta\delta$ has the mean field value 3/2. More explicitly, the trajectory of the branching point μ_* near μ_E is given by:

$$\mu_*(T) = \mu_E + c_1(T_E - T) + ic_2(T - T_E)^{\beta\delta} + \mathcal{O}((T - T_E)^2), \tag{22}$$

with some nonuniversal positive coefficients $c_{1,2}$. To derive this equation one observes that both t and h scaling variables are linear combinations of $(T - T_E)$ and $(\mu - \mu_E)$

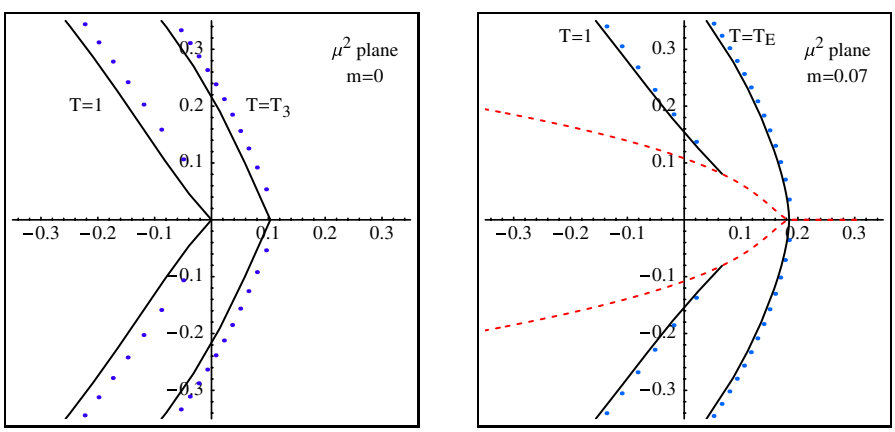

FIG. 4 (color online). Stokes boundaries and zeros of the $N = 120$ random matrix partition function at representative values of T at zero and nonzero quark mass. The trajectory of each branching point as a function of T is indicated by a dashed line.

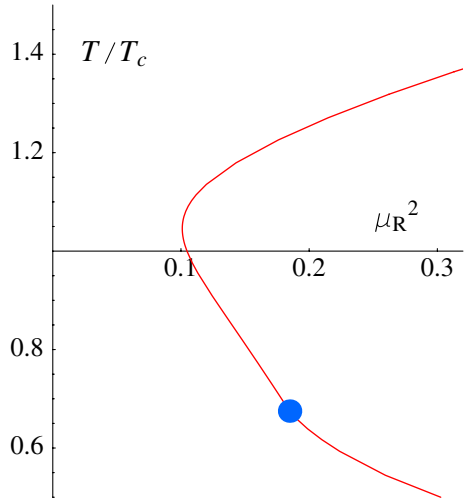

FIG. 5 (color online). The convergence radius μ_R^2 as a function of T in the random matrix model at $m = 0.07$ (7 MeV). The value of μ_R^2 is the distance of the singularity on the dashed line on Fig. 4 from the origin. The critical point at $T = T_E$ where the singularities pinch the real axis is shown.

and uses Eq. (13) for the branching point. The fact that the third term on the right-hand side in (22) is purely imaginary for $T > T_E$ is related to the fact that the branching point h_* in the h plane is on the imaginary axis for $t > 0$ as discussed in Sec. II D. Therefore

$$\mu_R^2(T) = |\mu_*(T)|^2 = \mu_E^2 + \tilde{c}_1(T_E - T) + \tilde{c}_2\theta(T_E - T)(T_E - T)^{\beta\delta} + \mathcal{O}((T - T_E)^2). \tag{23}$$

Below T_E, the singularity continues to move away from the origin, and the radius of convergence continues to increase. The radius is now determined by the spinodal point of the first order phase transition (but see discussion in the Appendix). This singularity resides on the continuation of the physical Riemann sheet under the cut.[2]

One must point out that the random matrix model of Ref. [4] does not capture a known feature of the QCD partition function—the periodicity, or invariance under the shift $\mu \to \mu + 2\pi i T$, which is due to the quantization of the baryon charge.[3] As shown by Roberge and Weiss [28] this periodicity is related to the appearance of a Stokes boundary given by $\mathrm{Im}\mu = \pi T$ for sufficiently high temperatures. For T of order 160 MeV, this Stokes boundary could interfere with convergence of the series only if the singularity we discuss moves further than $|\mu| \approx 500$ MeV.

[2]On a more subtle level, one has to note that the fact that the singularity (22) remains on the real axis is an artifact of the mean field critical behavior in the random matrix model ($\beta\delta = 3/2$). In QCD, the singularity moves off the real axis by an amount which scales as $(T_E - T)^{\beta\delta}$.

[3]A random matrix model which does capture this feature is studied in [27].

VI. SUMMARY AND DISCUSSION

We have described the location as well as temperature and quark mass dependence of the singularities of the QCD partition function in the complex μ plane. In the vicinity of the chiral phase transition at $m = 0$ the universality and scaling arguments predict that in the infinite volume the singularities are two complex conjugate branch cuts originating at a branching point on the real μ axis. The cuts are oriented at an angle to the negative μ axis given by (9). At nonzero m the branching points (and the cuts) are shifted in the direction given by angle $\psi \approx 48°$, by a distance of order $m^{0.54}$ (see Fig. 3).

A related consequence of the universal behavior of the complex T singularities, and the fact that $\psi < 90°$, is the prediction that the crossover point at $m \neq 0$, defined as the projection of the closest singularity onto the real axis, is *above* the second order O(4) line, as sketched in Fig. 1.

The singularities we describe determine the convergence of the Taylor expansion around the point $\mu = 0$. As a result, the radius of convergence ${\mu_R}^2$ at $T = T_c$ is limited by a singularity whose distance from the origin scales as ${\mu_R}^2 \sim m^{0.54}$, vanishing in the chiral limit. At $T = T_E$ the convergence radius $\mu_R(T)$ shows nonanalyticity described by Eq. (23).

The random matrix model of Ref. [4] illustrates these universal predictions: Figs. 4 and 5.

The knowledge of the complex plane singularities might be used to improve the Taylor expansion methods, for example, by constructing Padé or similar extrapolations [12], accommodating the correct universal singular behavior. It can also be used to crosscheck the results of lattice Monte Carlo simulations, by comparing the expected universal behavior of the partition function zeros to the output of a lattice calculation.

ACKNOWLEDGMENTS

This work was supported by the DOE Grant No. DE-FG0201ER41195, and by the Alfred P. Sloan Foundation.

APPENDIX A: TAYLOR EXPANSION NEAR A STOKES BOUNDARY

The following question has the practical importance for lattice Taylor expansion methods [8,10,12]: Does a Stokes boundary limit the convergence radius of a Taylor expansion and how? A view often expressed in the literature is that the thermodynamic functions can be analytically continued past the Stokes boundary (or a first order phase transition)—the true singularities being located at the branching points, where the Stokes boundaries end. Although this is correct in the strictly infinite volume $V = \infty$, this certainly is not correct for any finite volume, no matter how large. This must be so since the singularities of the free energy of the type $\log(z - z_k)$ are located along the Stokes boundaries. How then do these singularities appear

not to limit the radius of convergence in the $V \to \infty$ limit? The answer is that they do, but in order to see the divergence in the series, one needs to continue the expansion beyond some large order n_* which slides to infinity as $V \to \infty$. We determine n_* in this Appendix.

Consider a simplified problem, where the expansion point z_0 is located sufficiently close to the Stokes boundary so that the curvature of the boundary can be neglected, and the zeros can be considered equally spaced and extending to infinity. It is also convenient to transform the variable z to conformally map the Stokes boundary to the imaginary axis as shown in Fig. 6.

The contribution to the thermodynamic potential from the Stokes boundary at finite volume is the given by[4]

$$\Omega_{\rm sing} = -\log\left\{2Vz\prod_{k=1}^{\infty}\left[1-\left(\frac{zV}{\pi k}\right)^2\right]\right\} = -\log 2\sinh(zV)$$
$$= -zV - \ln(1-e^{-2zV}). \tag{A1}$$

We have also rescaled the variable z so that the spacing between zeros is π/V, to emphasize the fact the density of zeros grows linearly with V. In the thermodynamic limit

$$\frac{\Omega_{\rm sing}}{V} \xrightarrow{V\to\infty} \begin{cases} -z, & {\rm Re}z > 0; \\ z + i\pi, & {\rm Re}z < 0. \end{cases} \tag{A2}$$

On the Stokes boundary, ${\rm Re}z = 0$, ${\rm Re}\Omega$ is continuous but the normal derivative of ${\rm Re}\Omega$ is not, in accordance with the electrostatic analogy (6). However, the function $-z$ has no singularity on the Stokes boundary and can be analytically continued through it. Let us choose z_0 to be on the positive real axis and Taylor expand around such a point (see Fig. 6):

$$\Omega_{\rm sing}(z) - \Omega_{\rm sing}(z_0) = -(z-z_0)V + \sum_{n=1}^{\infty} a_n\left(\frac{z_0 - z}{z_0}\right)^n \tag{A3}$$

where

$$a_n = \frac{1}{n!}(2z_0V)^n\sum_{p=1}^{\infty} p^{n-1}e^{-2z_0Vp}. \tag{A4}$$

[4]A more common example $\Omega = -\log 2\cosh(zV)$ can be analyzed similarly, with a little additional complication, unnecessary for this discussion.

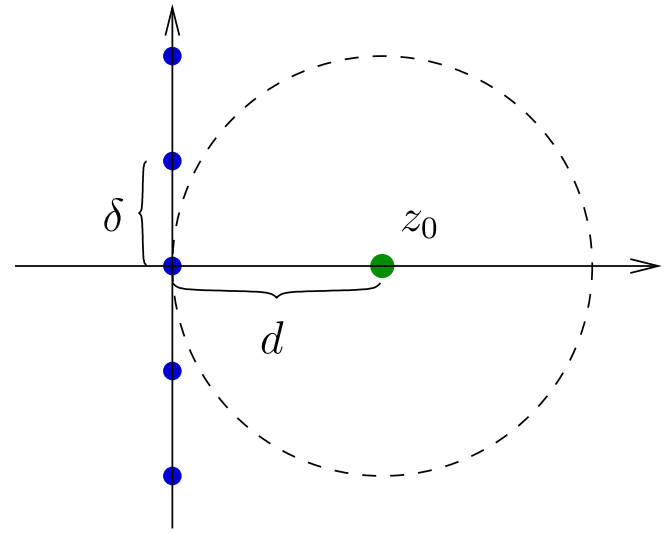

FIG. 6 (color online). The convergence disk of the Taylor series around point z_0 near a line of complex plane singularities.

For large V and n the coefficients approach[5]

$$a_n \xrightarrow{n\to\infty, V\to\infty} \begin{cases} e^{-n_*}(n_*)^n/n!, & n \ll n_* \equiv 2z_0V; \\ 1/n, & n \gg n_*. \end{cases} \tag{A5}$$

We see that the late terms $n > n_* \sim V$ will cause the divergence of the Taylor series outside the circle of radius $|z_0|$. The value of n_* can be written in terms of two quantities: the distance d of the expansion point from the Stokes boundary and the spacing δ between the zeros at the given volume (shown in Fig. 6). Recalling that in terms of the rescaled variable z the spacing is $\delta = \pi/V$ and the distance is $d = |z_0|$, we conclude:

$$n_* = \frac{2\pi d}{\delta}. \tag{A6}$$

[5]In the interval $n_* \ll n \ll n_*^2/(2\pi)$ the coefficients oscillate with maxima reaching $n_*/\sqrt{2\pi n^3}$ before settling on $a_n = 1/n$.

[1] M. Asakawa and K. Yazaki, Nucl. Phys. **A504**, 668 (1989).
[2] A. Barducci, R. Casalbuoni, S. De Curtis, R. Gatto, and G. Pettini, Phys. Lett. B **231**, 463 (1989); Phys. Rev. D **41**, 1610 (1990); A. Barducci, R. Casalbuoni, G. Pettini, and R. Gatto, Phys. Rev. D **49**, 426 (1994).
[3] J. Berges and K. Rajagopal, Nucl. Phys. **B538**, 215 (1999).
[4] M. A. Halasz, A. D. Jackson, R. E. Shrock, M. A. Stephanov, and J. J. M. Verbaarschot, Phys. Rev. D **58**, 096007 (1998).
[5] M. A. Stephanov, Prog. Theor. Phys. Suppl. **153**, 139 (2004); Int. J. Mod. Phys. A **20**, 4387 (2005).

[6] M. A. Stephanov, K. Rajagopal, and E. V. Shuryak, Phys. Rev. Lett. **81**, 4816 (1998); Phys. Rev. D **60**, 114028 (1999).
[7] Z. Fodor and S. D. Katz, J. High Energy Phys. 03 (2002) 014.
[8] C. R. Allton *et al.*, Phys. Rev. D **66**, 074507 (2002); **71**, 054508 (2005).
[9] P. de Forcrand and O. Philipsen, Nucl. Phys. **B642**, 290 (2002); **B673**, 170 (2003).
[10] R. V. Gavai and S. Gupta, Phys. Rev. D **71**, 114014 (2005).
[11] O. Philipsen, Proc. Sci., LAT2005 (2005) 016.
[12] M. P. Lombardo, Proc. Sci., LAT2005 (2005) 168.
[13] C. N. Yang and T. D. Lee, Phys. Rev. **87**, 404 (1952); T. D. Lee and C. N. Yang, Phys. Rev. **87**, 410 (1952).
[14] M. Fisher, in Lectures in Theoretical Physics Vol. 12C (University of Colorado Press, Boulder, 1965), p. 1.
[15] M. E. Fisher, Phys. Rev. Lett. **40**, 1610 (1978).
[16] C. Itzykson, R. B. Pearson, and J. B. Zuber, Nucl. Phys. **B220**, 415 (1983).
[17] M. A. Halasz, J. C. Osborn, M. A. Stephanov, and J. J. M. Verbaarschot, Phys. Rev. D **61**, 076005 (2000).
[18] K. Splittorff, hep-lat/0505001.
[19] S. Ejiri, Phys. Rev. D **73**, 054502 (2006).
[20] J. B. Kogut and M. A. Stephanov, Cambridge Monogr. Part. Phys., Nucl. Phys., Cosmol. **21**, 1 (2004).
[21] R. D. Pisarski and F. Wilczek, Phys. Rev. D **29**, 338 (1984).
[22] A. Pelissetto and E. Vicari, Phys. Rep. **368**, 549 (2002).
[23] D. Toussaint, Phys. Rev. D **55**, 362 (1997).
[24] A. D. Jackson and J. J. M. Verbaarschot, Phys. Rev. D **53**, 7223 (1996).
[25] M. A. Stephanov, Phys. Rev. Lett. **76**, 4472 (1996).
[26] M. A. Halasz, A. D. Jackson, and J. J. M. Verbaarschot, Phys. Lett. B **395**, 293 (1997).
[27] M. A. Halasz, hep-lat/0011086.
[28] A. Roberge and N. Weiss, Nucl. Phys. **B275**, 734 (1986).